Dynamics of the Lamellar−Cylindrical Transition in Weakly Segregated Diblock Copolymer Melts

J. L. Goveas*,† and S. T. Milner‡

Department of Chemical Engineering, Princeton University, Princeton, New Jersey 08544, and Exxon Research & Engineering, Route 22, East Annendale, New Jersey 08801

Received August 6, 1996; Revised Manuscript Received January 27, 1997[⊗]

ABSTRACT: We investigate the dynamics of the lamellar−cylindrical transition in weakly segregated diblock copolymer melts. We find the limit of stability of the lamellar phase with respect to the cylindrical phase and vice versa. We consider front propagation for stable phases invading metastable phases and compute the velocity and shape of such fronts close to coexistence.

I. Introduction

Diblock copolymers, which consist of two chemically different polymers (e.g. A and B) joined end to end, exhibit ordering transitions from the molten homogeneous state to various microphase-separated states. The simplest of these ordered phases are one-dimensional lamellae, hexagonally packed arrays of cylinders and body-centered cubic (bcc) arrays of spheres. Within the last decade, much experimental and theoretical work has been done toward understanding the thermodynamics of these transitions[1] but less has been done to address the associated dynamics. In this paper we consider the dynamics of transitions between these ordered phases and their stability relative to each other, focusing in particular on the transition between lamellar and cylindrical phases.

The diblock copolymer mean field phase diagram may be described by two parameters: χN, where N is the degree of polymerization of a single chain and χ is the Flory−Huggins parameter, and the relative composition of the two blocks (which we denote by f, the volume fraction of the A block). The order−disorder transition is known to be weakly first-order with a critical point at $f = 0.5$.[2] In the vicinity of the transition, the monomer concentration fluctuations become increasingly narrowly peaked around a single Fourier component, which we denote by q^*. At the limit of stability of the disordered phase, the order−disorder spinodal, $(\chi N)_s$, the fluctuations diverge on the sphere $||\vec{q}|| = q^*$.

Thus for asymmetrical copolymers where χN is close to $(\chi N)_s$, it is reasonable to describe the ordering transition by taking into consideration only the wave vectors with component q^*. This regime is known as the weak-segregation limit and produces an ordered phase with periodicity $2\pi/q^*$, which is on the order of the radius of gyration of the copolymers.[2] The mean-field weak-segregation diblock copolymer phase diagram is shown in Figure 1, including the order−disorder phase boundary and the phase boundaries between the three ordered phases described above. [We do not show the gyroid phase since it cannot be accounted for within the one-harmonic prescription described above. However, since there is a window of stability for the gyroid phase between lamellae and cylinders,[3] our analysis is not valid in the region where such an intervening phase is present.]

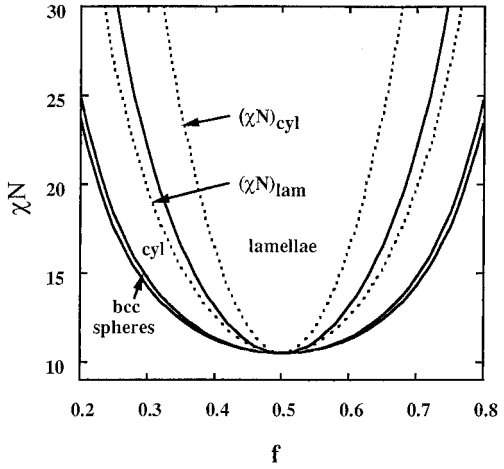

Figure 1. Mean-field phase diagram, showing where lamellae, cylinders, and bcc spheres exist as equilibrium phases.[2] We also show the lamellar−cylindrical order−order spinodals.

We expect to find spinodals flanking each side of the lamellar−cylindrical boundary, $(\chi N)_{lc}$, marking the limit of stability of the corresponding ordered phases. Defining the distance in χN from the order−disorder spinodal as $x = \chi N - (\chi N)_s$, we denote the value of x where lamellae become unstable and spontaneously form cylinders by x_{lam}, and where cylinders become unstable and spontaneously form lamellae by x_{cyl}.

We will also be concerned with the evolution of one ordered phase into another ordered phase. Suppose we have prepared an equilibrium lamellar phase which we then quench into a state where the hexagonal phase is stable ($x < x_{lc}$). If the lamellar phase is unstable in this regime ($x < x_{lam}$), fluctuations of cylindrical order will grow spontaneously and exponentially, and we expect that the growth kinetics will be of the Cahn−Hilliard type. On the other hand, if we quench less deeply so that the lamellar phase is metastable, $x_{lc} < x < x_{lam}$, fluctuations will nucleate the cylindrical phase inside the lamellar phase. The stable cylindrical phase then invades the lamellar phase by means of a propagating front which leaves behind in its wake cylindrical order. We shall describe this front propagation by finding the shape of the front and calculating its velocity. Using similar arguments, we will also consider the converse transition of quenching a cylindrical phase into a more stable lamellar phase.

One phase can evolve into another through many different pathways. An obvious pathway for the lamellar−cylindrical transition is suggested by the fact that the set of wave vectors that characterize lamellar order

† Princeton University. Present address: Materials Research Laboratory, University of California, Santa Barbara, CA 93106-5130.
‡ Exxon Research & Engineering.
⊗ Abstract published in *Advance ACS Abstracts,* April 1, 1997.

S0024-9297(96)01181-3 CCC: $14.00

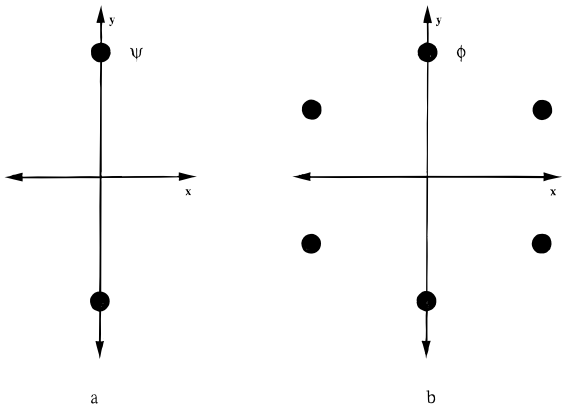

Figure 2. Set of wave vectors characterizing (a) lamellar and (b) cylindrical order.

in reciprocal space is a subset of those that form the cylindrical phase (see Figure 2). Consequently, it is reasonable to suppose that cylinders are formed by modulating lamellae, i.e. by the growth of four additional Bragg peaks. Likewise, cylinders may be converted into lamellae by simultaneous dimming of these same peaks and brightening of the peaks at $\pm q^*\vec{y}$.

We organize this paper as follows: in Section II we develop a free energy expansion for phases with both lamellar and cylindrical order, which enables us to calculate the order−order spinodals on either side of the lamellar−cylindrical boundary in Section III; Section IV deals with front propagation close to coexistence, and we discuss the velocity and shape of the front in Sections VI and V. We conclude and make some comments in Section VII.

II. Free Energy Expansion

The local free energy density functional for any ordered phase may be written (following Leibler[2]) as a power series in the order parameter:

$$F = F_o + k_b T \sum_{m=2}^{\infty} V^{-m} \frac{1}{m!} \sum_{\vec{q}_1,\ldots,\vec{q}_m} \Gamma_m(\vec{q}_1, \ldots, \vec{q}_m)\Psi(\vec{q}_1)\ldots\Psi(\vec{q}_m) \quad (1)$$

The coefficients Γ_m are related to the correlation functions which are calculated using the random phase approximation (RPA) and are functions of f only, and V is the volume of the copolymer system. Since we are close to the order−disorder transition we keep only terms up to fourth order in the order parameter Ψ.

We consider a two-parameter family of ordered phases which may be created by superposing lamellar and cylindrical order. For such a phase we construct an order parameter:

$$\Psi(\vec{r}) = \psi\{\exp(i\vec{Q}_1\vec{r}) + \text{cc}\} + \frac{\phi}{\sqrt{3}} \sum_{m=1}^{3} \{\exp(i\vec{Q}_{2m}\vec{r}) + \text{cc}\} \quad (2)$$

The sets $\{\vec{Q}_1\}$ and $\{\vec{Q}_{2m}\}$ contain the wave vectors for lamellar and cylindrical order respectively. The amplitude of the lamellar phase is given by ψ and that of the cylindrical phase by ϕ. For $\phi = 0$ we recover pure lamellar order and similarly setting $\psi = 0$ gives us pure cylindrical order, whereas non-zero values of ψ and ϕ produce order intermediate between lamellar and cylindrical. (We have taken the relative phases of the cylindrical waves to be the same as those for equilibrated cylinders.[2])

Substituting the expression for the order parameter, eq 2, into eq 1 and expanding up to fourth order in both amplitudes gives us an expression for the local free energy for the restricted set of configurations above as a polynomial in ψ and ϕ:

$$F(\psi,\phi)N/k_B T = (\psi^2 + \phi^2 + a\psi\phi)(-2x) + b\left(\phi^2\psi + \frac{1}{\sqrt{3}}\phi^3\right) + c_1\left(\psi^4 + \frac{4}{\sqrt{3}}\psi^3\phi\right) + c_2(\psi^2\phi^2) + c_3\left(\psi\phi^3 + \frac{\sqrt{3}}{4}\phi^4\right) \quad (3)$$

Henceforth we will take $k_B T$ to be unity.

We recall that the $\Gamma_n(\vec{q}_1\ldots\vec{q}_n)$s vanish unless the wave vectors $\{\vec{q}_1\ldots\vec{q}_n\}$ sum to zero. The calculation of the coefficients a, b, c_1, c_2, and c_3) is then a simple counting of these vanishing sums for each of the terms in eq 3 using wave vectors from the sets $\{\vec{Q}_1\}$ and $\{\vec{Q}_{2m}\}$. For example, a term of order $\phi^2\psi$ corresponds to a choice of two wave vectors from among $\{\vec{Q}_{2m}\}$ and one from among $\{\vec{Q}_1\}$. The restriction that these wave vectors sum to zero dictates the type and number of terms that appear.

The numerical prefactors of the amplitudes (unity for ψ and $1/\sqrt{3}$ for ϕ) are chosen for convenience so that the coefficients of the second-order terms in the expansion are equal. With this convention, we find $a = 2/\sqrt{3}$.

For the cubic terms we must count the number of triangles that can be made by summing three wave vectors at a time. Since the wave vectors are equal in magnitude within the weak segregation approximation, the triangles so formed are always equilateral. We find that $b = {}^2/_3\Gamma_3$. (Note that the terms of order ψ^3 and $\psi^2\phi$ are absent as it is not possible to form triangles using less than two vectors from $\{\vec{Q}_{2m}\}$.)

However, for the coefficients of the quartic terms, even with all $|\vec{q}_i|$ equal, there are extra degrees of freedom that correspond to the two independent angles that exist between four $\vec{q}_i$s that sum to zero. We follow the same convention as Leibler to express these two angles: $\Gamma_4(\vec{q}_1, \vec{q}_2, \vec{q}_3, \vec{q}_4) = \Gamma_4(h_1, h_2)$ where h_1 and h_2, which determine the two independent angles, are defined by

$$||\vec{q}_1 + \vec{q}_2||^2 = h_1 q^{*2}$$

$$||\vec{q}_1 + \vec{q}_4||^2 = h_2 q^{*2}$$

Since $||\vec{q}_1 + \vec{q}_2||^2 = ||\vec{q}_3 + \vec{q}_4||^2 = ||\vec{q}_1 + \vec{q}_4||^2 = ||\vec{q}_2 + \vec{q}_3||^2$ this enforces the relation

$$\Gamma_4(h_1, h_2) = \Gamma_4(h_1, 4 - h_1 - h_2) = \Gamma_4(h_2, 4 - h_1 - h_2)$$

We find for the quartic coefficients

$$c_1 = \frac{1}{4}\Gamma_4(0, 0) \quad (4)$$

$$c_2 = \frac{1}{2}\Gamma_4(0, 0) + \frac{2}{3}\Gamma_4(0, 1) \quad (5)$$

$$c_3 = \frac{1}{3\sqrt{3}}[\Gamma_4(0, 0) + 4\Gamma_4(0, 1)] \quad (6)$$

III. Spinodals

A thermodynamically stable phase corresponds to a local minimum in the free energy. Since the free energy

is convex in the vicinity of the minimum, the symmetric matrix of its second partial derivatives, the "Hessian", must have positive eigenvalues. The phase becomes unstable as soon as any of the eigenvalues vanish, corresponding to the vanishing of the determinant of the Hessian.

Let us first consider fluctuations about the pure lamellar phase. The onset of instability is then given by:

$$\det\left|\begin{matrix}\frac{\partial^2 F}{\partial\psi^2} & \frac{\partial^2 F}{\partial\psi\partial\phi}\\ \frac{\partial^2 F}{\partial\phi\partial\psi} & \frac{\partial^2 F}{\partial\phi^2}\end{matrix}\right|_{\psi=\psi_{\min},\phi=0} = 0$$

where $\psi_{\min}$ is the equilibrium amplitude of the lamellar order parameter such that

$$\left.\frac{\partial F}{\partial\psi}\right|_{\phi=0} = 0 \tag{7}$$

Using our expression for the local free energy density we find that the lamellar phase at fixed f becomes unstable when

$$x_{\text{lam}} = \frac{\frac{1}{4}\Gamma_3{}^2\Gamma_4(0,0)}{\left[-\frac{1}{2}\Gamma_4(0,0)+\Gamma_4(0,1)\right]^2} \tag{8}$$

with an amplitude

$$\psi_s = \frac{-\Gamma_3}{-\frac{1}{2}\Gamma_4(0,0)+\Gamma_4(0,1)} \tag{9}$$

The analogous equation set for the cylindrical spinodal is

$$\det\left|\begin{matrix}\frac{\partial^2 F}{\partial\psi^2} & \frac{\partial^2 F}{\partial\psi\partial\phi}\\ \frac{\partial^2 F}{\partial\phi\partial\psi} & \frac{\partial^2 F}{\partial\phi^2}\end{matrix}\right|_{\phi=\phi_{\min},\psi=0} = 0$$

where the equilibrium cylindrical amplitude satisfies

$$\left.\frac{\partial F}{\partial\phi}\right|_{\psi=0} = 0 \tag{10}$$

The location of the spinodal and the corresponding amplitude of the cylindrical phase are then

$$x_{\text{cyl}} = \frac{\sqrt{3}}{4}\phi_s[b + c_3\phi_s] \tag{11}$$

$$\phi_s = \frac{-\sqrt{3}\Gamma_3}{-\frac{1}{2}\Gamma_4(0,0)+\Gamma_4(0,1)} \tag{12}$$

Figure 1 shows a plot of the lamellar−cylindrical boundary and the two order−order spinodals as a function of f and χN.

We may ask in what direction in the parameter space $\{\psi,\phi\}$ the lamellar and cylindrical phases become unstable. If we write the unstable eigenvector of the Hessian as $[1,\alpha]$ in $\{\psi,\phi\}$ space, α can be determined by requiring

$$\begin{bmatrix}\frac{\partial^2 F}{\partial\psi^2} & \frac{\partial^2 F}{\partial\psi\partial\phi}\\ \frac{\partial^2 F}{\partial\phi\partial\psi} & \frac{\partial^2 F}{\partial\phi^2}\end{bmatrix}\begin{bmatrix}1\\ \alpha\end{bmatrix} = 0$$

A short calculation tells us that both the lamellar and hexagonal phases become unstable in the direction $[1, -1/\sqrt{3}]$ in ψ,ϕ space.

IV. Front Propagation

We now consider the problem of a front propagating between two phases that are close to coexistence. The system evolves in time by means of an interface that moves in space into a higher energy state from a lower energy one. We describe the front in terms of the two scalar order parameters, ψ and ϕ, which are the local amplitudes of the lamellar and cylindrical concentration profiles. Since ψ and ϕ are not conserved variables, we may write dynamical equations for them having the form (see, for example, ref 4):

$$\Gamma\frac{d\psi}{dt} = -\frac{\delta H}{\delta\psi} \tag{13}$$

$$\Gamma\frac{d\phi}{dt} = -\frac{\delta H}{\delta\phi} \tag{14}$$

The right hand side of the equations shows that the ψ and ϕ profiles relax locally in reponse to the themodynamically conjugate potential. The energy released by the system in reducing its free energy is dissipated by drag forces where Γ is a "drag coefficient". For simplicity we have neglected off-diagonal Onsager coefficients.

We express the effective Hamiltonian H as a sum of two types of terms, a local part which we have already derived and square gradient terms reflecting the free energy cost to create interfaces in the system.

$$H = k_B T\int\frac{d^3r}{v}[a_o{}^2(\nabla\psi)^2 + a_o{}^2(\nabla\phi)^2 + F(\psi,\phi)] \tag{15}$$

where a_o is a monomeric length and v is a monomeric volume.

In writing eq 15, we have made the simplest possible assumptions about the gradient terms; namely, that they are (i) second order in wave vector, (ii) isotropic, and (iii) second order in the amplitudes and (iv) that all cross terms mixing $\nabla\psi$ and $\nabla\phi$ vanish.

The most serious of these assumptions are the first two. It has been argued[5] that for amplitude modulations of a lamellar phase transverse to the layering direction, the gradient terms should begin at fourth order. We discuss this point in the Appendix. To summarize our conclusion there, it is a reasonable approximation to take square-gradient terms in all directions, unless we are very close to the critical point. These need not be isotropic, but it is a simple matter to generalize our results to anisotropic square-gradient terms (in effect, the value of a_0 would depend on the direction of the interface normal with respect to the layering direction).

We estimate Γ by applying eq 13 to the relaxation of a lamellar fluctuation in the disordered phase which has the form $\exp[4xt/(\Gamma\nu N)]$ (since we are in weak segregation). If we consider a disordered phase for which χN is zero, the dynamics are simply those of homopolymer

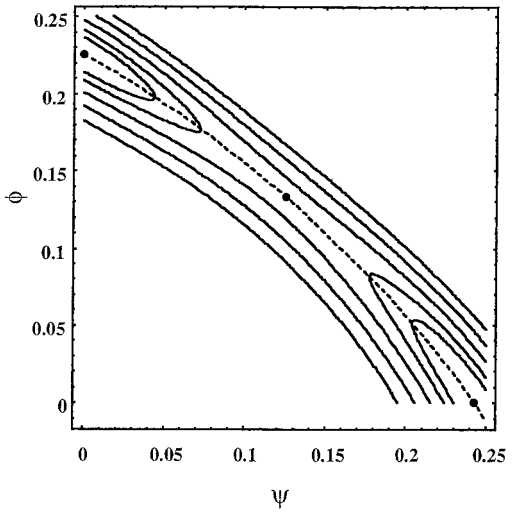

Figure 3. Contour plot of $F(\psi,\phi)$ at coexistence for $f = 0.3$. Contours with values −0.43, −0.425, −0.415, −0.4, and −0.38 are shown. Circles indicate the two minima at (ψ_{min}, 0) and (0, ϕ_{min}) and the saddle point (ψ^*,ϕ^*) between them. The dashed line is $\phi_c(\psi)$, a close approximation to the path of steepest descent.

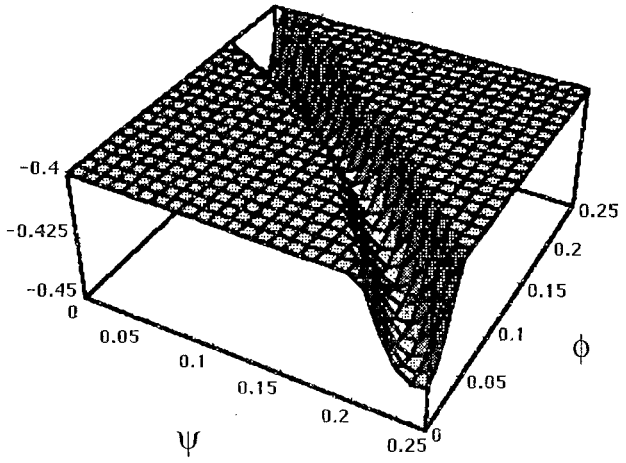

Figure 4. Free energy, $F(\psi,\phi)$, at coexistence for $f = 0.3$, which has a deep, narrow channel between coexisting minima. The free energy surface has been truncated as a visual aid; in reality it rises steeply beyond the channel walls.

chains. For unentangled chains, the relaxation time in the homogeneous melt is given by the Rouse time τ_{Rouse}, and by the reptation time τ_d for entangled chains.[6] Correspondingly we can set $\Gamma = 4(\chi N)_s\tau_{Rouse}/\nu N$ or $\Gamma = 4(\chi N)_s\tau_d/\nu N$. [A more accurate calculation for Γ for disordered diblock copolymers can be found in ref 7 for entangled polymers and ref 8 for unentangled copolymers.] Weak cylindrical perturbations of the disordered phase ought to relax in the same way as weak lamellar fluctuations (since within linear response the cylindrical perturbation is a superposition of three lamellar waves) so we use the same "drag" coefficient for both ψ and ϕ.

At coexistence, there is no front motion so that the equations for the shape of the front become

$$0 = 2a_o^2 \frac{d^2\psi}{dz^2} - \frac{\partial F}{\partial \psi} \tag{16}$$

$$0 = 2a_o^2 \frac{d^2\phi}{dz^2} - \frac{\partial F}{\partial \phi} \tag{17}$$

In principle we can solve this coupled set for the functional form of $\psi(z)$ and $\phi(z)$, where the shape of the interface minimizes the free energy. We can think of the path of the front in its evolution from one state to another as some trajectory in $\{\psi,\phi\}$ space. Consequently it is convenient to parametrize the trajectory in ϕ and consider that the front moves along a one-dimensional curve in $\phi(\psi)$ (or vice versa) between the two stable points, $\{\psi_{min},0\}$ and $\{0,\phi_{min}\}$, so that we do not have to make reference to the underlying spatial variable z.

The local free energy density in $\{\psi,\phi\}$ space close to coexistence is shown as a contour plot in Figure 3 and as a 3-D plot in Figure 4. Notice that there are three extrema in the landscape: a minimum along the ψ-axis corresponding to pure lamellar order, a minimum along the ϕ-axis for pure cylindrical order, and a saddle point that lies between them. The surface itself exhibits a narrow deep channel connecting the two minima and the saddle point. The curve $\phi(\psi)$ corresponding to the front must lie close to the "bottom" of this channel (the path of steepest descent) since deviations away from the bottom quickly incur a large increase in the local free energy $F(\psi,\phi)$ with little reduction of the gradient free energy. The saddle point represents the most significant free energy barrier in the channel and its free energy relative to that of the coexisting phases determines the width of the front.

We will now make several approximations to the free energy landscape. We have numerically computed a path $\phi_c(\psi)$ in $\{\psi,\phi\}$ that closely approximates the path of steepest descent as the solution to the cubic

$$\left.\frac{\partial F}{\partial \phi}\right|_{\phi_c(\psi)} = 0 \tag{18}$$

This path is shown in Figure 3. From its definition, it must pass through the saddle point and the two minima corresponding to the stable phases. It is a good approximation to the path of steepest descent because the curvature of the free energy surface is so much larger across the channel than along it.

We note that the path of steepest descent is nearly a straight line in $\{\psi,\phi\}$ space, which suggests approximating the function $\phi_c(\psi)$ by a straight line connecting the two minima

$$\phi_l(\psi) = -\frac{\phi_{min}}{\psi_{min}}\psi + \phi_{min} \tag{19}$$

We observe (see Figure 5) that at coexistence the free energy along the path of steepest descent is very nearly a symmetric quartic which allows us to write in an excellent approximation

$$F(\psi) - F(\psi_{min}) = \frac{C}{N}\left[1 - \left(\frac{2\psi}{\psi_{min}} - 1\right)^2\right]^2 \tag{20}$$

where we have used the simple straight line path $\phi_l(\psi)$ in eq 3. In order that the free energy along this path varies as $F(\psi,\phi_c(\psi))$ we determine the coefficient C by requiring eq 20 to give the free energy at the saddle point $F(\psi^*,\phi^*)$:

$$C = N\frac{F(\psi^*,\phi^*) - F(\psi_{min}, 0)}{\left[1 - \left(\frac{2\psi^*}{\psi_{min}} - 1\right)^2\right]^2} \tag{21}$$

We would like to obtain a simple expression for the free

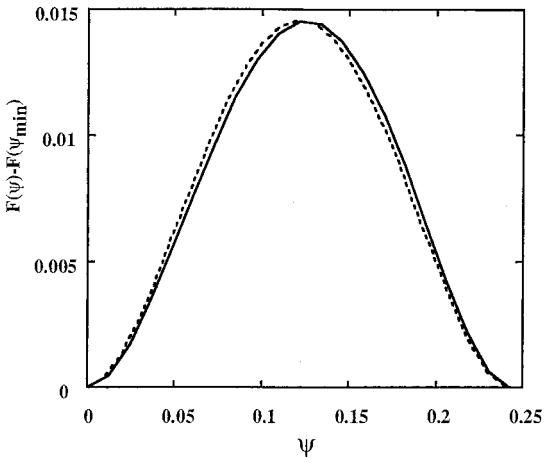

Figure 5. $F(\psi) - F(\psi_{min})$ evaluated along the steepest descent path of Figure 3 (solid curve) is well approximated by a quartic (dashed curve).

energy at the saddle point. At any χN, the simultaneous solution of $\partial F/\partial\psi = 0$ and $\partial F/\partial\phi = 0$ gives us the saddle point. Let us make the ansatz that ϕ^* is a linear function of ψ^*, but since the saddle point is annihilated at each spinodal, the relation between ψ^* and ϕ^* is necessarily

$$\phi^* = -\frac{\phi_s}{\psi_s}\psi^* + \phi^s \tag{22}$$

Since $\phi_s/\psi_s = \sqrt{3}$, the slope of eq 3 reflects the direction in which the ordered phases become unstable (see Section III). Substituting eq 22 into $\partial F/\partial\psi = 0$, we get a simple quadratic with the solution

$$\psi^* = \frac{\phi_s}{\sqrt{3}} - 2\left[\frac{\phi_s(x - x_{lam})}{\sqrt{3}z_3}\right]^{1/2} \tag{23}$$

$$\phi^* = 2\left[\frac{\sqrt{3}\phi_s(x - x_{lam})}{z_3}\right]^{1/2} \tag{24}$$

So we have the interesting result that $\phi^* \sim (x - x_{lam})^{1/2}$ at all χN. (Substituting the ansatz (eq 22) into the second equation of the coupled set $\partial F/\partial\phi = 0$, gives us the quadratic above times a linear function of ψ, showing that the ansatz solves the equation set exactly.)

We substitute these results into eq 3 and find after some algebra

$$F(\psi^*, \phi^*) - F(\psi_{min}, 0) = \frac{1}{N}(x - x_{lam})^2\Omega \tag{25}$$

where

$$\Omega = 4\left[\frac{1}{\Gamma_4(0, 0)} - \frac{1}{\Gamma_4(0, 1) + \frac{1}{2}\Gamma_4(0, 0)}\right] \tag{26}$$

V. Front Velocity

If we assume that the front is propagating with a constant velocity, so that $\psi = \psi(z - vt)$ and $\phi = \phi(z - vt)$, eqs 13 and 14 become

$$-\Gamma v\frac{d\psi}{dz} = \frac{2a_o^2}{\nu}\frac{d^2\psi}{dz^2} - \frac{1}{\nu}\frac{\partial F}{\partial\psi} \tag{27}$$

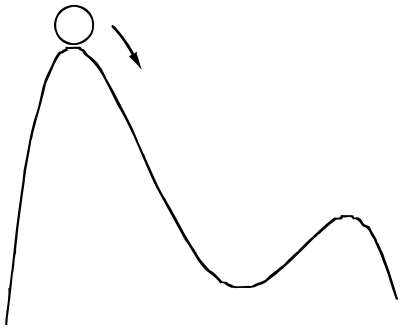

Figure 6. Newtonian particle moving in an external field analogous to eq 29 for front propagation.

$$-\Gamma v\frac{d\phi}{dz} = \frac{2a_o^2}{\nu}\frac{d^2\phi}{dz^2} - \frac{1}{\nu}\frac{\partial F}{\partial\phi} \tag{28}$$

Let us first consider for simplicity the case of front propagation with only one order parameter, η.

$$-\Gamma v\frac{d\eta}{dz} = \frac{2a_o^2}{\nu}\frac{d^2\eta}{dz^2} - \frac{1}{\nu}\frac{dF}{d\eta} \tag{29}$$

This equation also describes a classical particle of mass $2a_o^2/\nu$ moving in an inverted potential $-F(\eta)$ with two maxima at η_1 and η_2 (see Figure 6), with friction coefficient Γv. Here z plays the role of time, and η is the particle position. The initial condition corresponding to a nearly constant value of the order parameter at a minimum of $F(\eta)$ far removed from the front is a particle starting with infinitesimally small velocity at a very early time.

On physical grounds, there is only one value of friction coefficient Γv that will dissipate the kinetic energy gained as the particle falls from the higher maximum $-F(\eta_1)$ to rest at the lower maximum $-F(\eta_2)$.

Our system with two order parameters likewise corresponds to a particle moving with friction in a two-dimensional potential $-F(\psi,\phi)$. Fixing the free energy difference between states in our system consequently selects a unique velocity at which a front will propagate.

Multiplying eq 27 by $d\psi/dz$ and eq 28 by $d\phi/dz$ and adding them together gives us

$$-\Gamma v\left[\left(\frac{d\psi}{dz}\right)^2 + \left(\frac{d\phi}{dz}\right)^2\right] = \frac{1}{\nu}\frac{d}{dz}\left[a_o^2\left(\frac{d\psi}{dz}\right)^2 + a_o^2\left(\frac{d\phi}{dz}\right)^2 - F(\psi,\phi)\right] \tag{30}$$

We now proceed for a cylindrical phase invading a lamellar phase (so that $\psi = 0$, $\phi = \phi_{min}$ at $z = -\infty$ and $\psi = \psi_{min}$, $\phi = 0$ at $z = \infty$), but our final results may also be used for the case of a lamellar phase invading a cylindrical phase. We integrate both sides of eq 30 in z, and recognize that gradients are small far from the interface ($z = 0$). Then we get for the velocity of the front

$$v = \frac{1}{\nu}\frac{[F(\psi_{min}, 0) - F(0, \phi_{min})]}{\Gamma\int_{-\infty}^{\infty} dz\left[\left(\frac{d\psi}{dz}\right)^2 + \left(\frac{d\phi}{dz}\right)^2\right]} \tag{31}$$

As we are near coexistence, we can simplify the kernel in the denominator by integrating eq 30 with $v = 0$ to give

$$a_o^2\left[\left(\frac{d\psi}{dz}\right)^2 + \left(\frac{d\phi}{dz}\right)^2\right] = F(\psi, \phi) - F(\psi_{min}, 0) \quad (32)$$

Using our ansatz for the path of the front and changing the integration variable from z to ψ then allows us to approximate the integral as

$$\int_{-\infty}^{\infty} dz\left[\left(\frac{d\psi}{dz}\right)^2 + \left(\frac{d\phi}{dz}\right)^2\right] \approx \int_0^{\psi_{min}} d\psi \frac{1}{a_o}\left[(F - F(\psi_{min}, 0))\left(1 + \left(\frac{\phi_{min}}{\psi_{min}}\right)^2\right)\right]^{1/2} \quad (33)$$

We then use eq 20 to evaluate this integral which gives us for the velocity:

$$v = \frac{a_o N^{1/2}}{\Gamma\nu} \frac{3[F(\psi_{min}, 0) - F(0, \phi_{min})]}{2[C(\psi_{min}^2 + \phi_{min}^2)]^{1/2}} \quad (34)$$

In order to estimate the front velocity close to coexistence, we evaluate all terms in eq 34 at coexistence with the exception of $F(\psi_{min},0) - F(0,\phi_{min})$ which we expand about its value at coexistence so

$$F(\psi_{min}, 0) - F(0, \phi_{min}) = 0 + \frac{2(x - x_{lc})\left(\phi_{min,lc}^2 - \frac{x_{lc}}{c_1}\right)}{N} \quad (35)$$

where by $\phi_{min,lc}$ we wish to indicate the amplitude of the cylindrical minimum at coexistence. Substituting eqs 35 and 25 into eq 34 gives us the final result for the velocity as

$$v = \frac{a_o}{\Gamma\nu N^{1/2}} \frac{3[\chi N - (\chi N)_{lc}][\phi_{min,lc}^2 - (x_{lc}/c_1)]}{[C(\psi_{min,lc}^2 + \phi_{min,lc}^2)]^{1/2}} \quad (36)$$

Using the results of refs 7 and 8 for Γ, we can write this velocity as

$$v \approx \frac{R}{\tau}[\chi N - (\chi N)_{lc}]g(f) \quad (37)$$

where R is the root-mean-square end-to-end distance of the chain and τ is the relaxation time which depends on the molecular weight of the chain. The velocity is then linear in the distance from coexistence in χN times a factor $g(f)$, which depends only on the volume fraction f and scales as R/τ. Figures 7 and 8 show the dimensionless velocity as a function of f for values of χN that are 15% of $(\chi N)_{lc} - (\chi N)_{lam}$ away from coexistence for unentangled and entangled chains respectively. We see that the velocity decreases monotonically to zero at the critical point where there is no driving force for front motion. We have estimated the velocity scale for an unentangled polystyrene-polyvinylpyridine (PS−PVP) diblock copolymer and an entangled polyethylenepropylene−polyethylenethylene (PEP−PEE) copolymer close to their ordering transitions using the self-diffusion data of Lodge et al.[9,10] We find velocity scales on the order of a few ångstroms per second and micrometers per second respectively, the difference being mainly due to the large friction coefficient of PS (high T_g). Thus careful choice of copolymer ought to make the velocity experimentally accessible.

VI. Shape of the Front

We will now describe the shape of the front near coexistence. Using the quartic eq 20 for the free energy

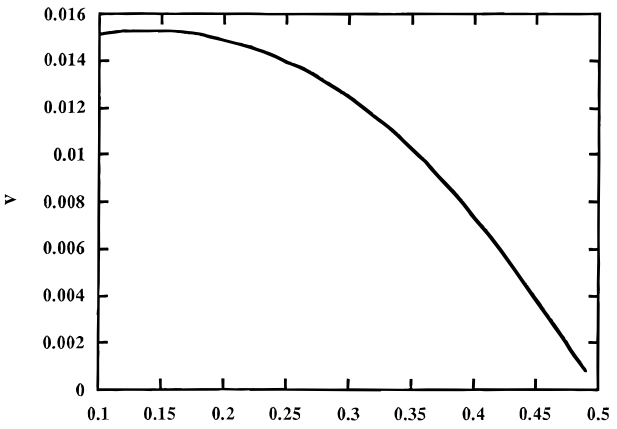

Figure 7. Velocity scaled by (R/τ_{Rouse}) as a function of volume fraction, f, for unentangled chains.

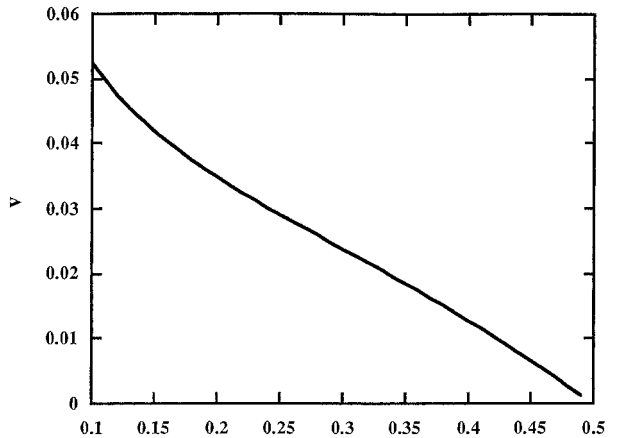

Figure 8. Velocity scaled by (R/τ_d) as a function of volume fraction, f, for entangled chains.

and our linear ansatz $\phi_l(\psi)$ for the path of the front, we can easily solve eq 32 to give the usual hyperbolic tangent profile for the front

$$\psi(z) = \psi_{min}\frac{1}{1 + e^{-z/W}} \quad (38)$$

$$\phi(z) = \phi_{min}\frac{e^{-z/W}}{1 + e^{-z/W}} \quad (39)$$

where

$$W = R\left[\frac{\psi_{min}^2 + \phi_{min}^2}{16C}\right]^{1/2} \quad (40)$$

The width of the front diverges at the critical point as we expect since $\psi_{min} \sim (f - 1/2)$, $\phi_{min} \sim (f - 1/2)$, and $C \sim (f - 1/2)^4$ in the limit of $f \to 1/2$, where we have used the result that $\Gamma_3 \sim (f - 1/2)$ while Γ_4 is $O(1)$.

VII. Conclusions

We have considered the dynamics of the lamellar−cylindrical transition in weakly-segregated diblock copolymer melts. We have calculated spinodals where lamellae and cylinders become unstable on either side of the phase boundary. Since growth of the stable phase ought to proceed by qualitatively different mechanisms

on either side of the spinodal (by Cahn−Hilliard kinetics beyond the spinodal and by front propagation in the metastable regime), it should be possible to monitor the growth of order using SANS after quenching and so map out the spinodals to compare with our predictions. A qualitative feature of our phase diagram is that the lamellar phase is metastable over a much narrower region of χN than the cylindrical phase.

We have estimated the velocity of a propagating front near coexistence and find that for fixed f it scales linearly with distance in χN from the lamellar−cylindrical phase boundary. We also predict how this velocity should depend on N and f and identify a characteristic scale R/τ. We use a simple approximate form for the relation between lamellar and cylindrical order parameters and consequently find that the shape of the front may be described as a hyberbolic tangent. Some of these aspects of front propagation should be directly observable by making temperature jumps across the phase boundary and using optical microscopy with crossed polarizers to detect front motion.

We point out that since our calculation is done close to the order−disorder transition, fluctuation effects are significant.[11,12] However mean-field theory is more reliable as the copolymer becomes more asymmetrical. Experimental comparison with our theory would be most appropriate in this part of the phase diagram.

We have not solved any of our dynamical equations exactly, which would involve a numerical solution of coupled sets of partial differential equations. These calculations might be interesting for copolymers far from coexistence—for example in the vicinity of the order−order spinodals (where the front velocity should still be finite since the free energy difference between phases is always finite).

We have simplified our calculations by focusing on a restricted set of fluctuations, which are subsets of the wave vectors of the lamellar and cylindrical phases. This choice is partly motivated by experimental observation of modulated lamellae in the early kinetics of the lamellar−cylindrical transition. If the ordered phases evolve by modulations which are unrelated to the existing structures it can be shown that all cross terms, except for the $\psi^2\phi^2$ term, in the local free energy are absent and that the free energy barrier between the phases is in fact higher. In addition, there are some fluctuations such as those leading to more exotic intermediate configurations such as catenoid−lamellar structures which simply cannot be described within the framework of the one-harmonic approximation.

Our methods may be applied to transitions between other ordered phases which exhibit epitaxy. Recently Qi and Wang have explored transitions between bcc and cylindrical phases[13] using methods similar to ours. Fredrickson and Binder[14] have considered the case of nucleation of lamellar phases from the disordered phase which involves the incorporation of fluctuation corrections.

We have also left other interesting questions unexplored, such as the effect of anisotropy in gradient terms on front propagation, which are important in creating a more realistic description of the dynamics. These should affect both the front velocity and the widths of the profiles anisotropically. Recent experiments by Dai et al.[15] have observed grains of cylindrical phases growing out of disorder, where the grains grow preferentially in the direction parallel to the cylinder axis. We expect similar anisotropy in lamellar−cylindrical transitions, both in the front velocity and in the front widths.

Acknowledgment. This work was supported primarily by the MRSEC program of the National Science Foundation under Award No. DMR-9400362. We thank W. B. Russel for suggesting this problem to us and G. H. Fredrickson for useful discussions.

Appendix

Let us consider a scalar field that orders at a prescribed wavenumber with no preference as to the direction of ordering. The gradient terms in the Brazovskii Hamiltonian[11,12] may then be written

$$H = \int \mathrm{d}V\,[(\nabla^2 + q_0^2)\Psi]^2 \tag{A1}$$

where $\Psi(x)$ is a modulated concentration wave

$$\Psi(x) = a(x)\exp(i\vec{q}_0\cdot x) \tag{A2}$$

in which the modulation of $a(x)$ is assumed to be "slow", that is to say $a(x)$ varies on a length scale much larger than q_0^{-1}.

Substituting eq A2 into eq A1 and performing a gradient expansion leads to

$$H \approx \int \mathrm{d}V[4((\vec{q}_0\cdot\nabla)a)^2 + (\nabla^2 a)^2] \tag{A3}$$

This result suggests[5] that the only nonvanishing square gradient term is for "longitudinal" amplitude modulations, i.e. with the modulation wave vector parallel to the ordering wave vector $\vec{q}_0$.

Indeed, a similar argument applied to *phase* modulations of $\Psi(x)$ establishes the particular anisotropic form of smectic elasticity.[16] In this case, the argument can be made quite generally on the grounds of the invariance of the energy of a lamellar phase under rotations.

However, eq A3 was derived from a quadratic Hamiltonian, which invites the question of whether or not eq A3 can be justified on more general grounds of rotational invariance. In order to answer this question, we find it useful to examine eqs A2 and A1 in Fourier space.

The quadratic Hamiltonian given by eq A1 in Fourier space is

$$H = \int \mathrm{d}q(q^2 - q_0^2)\Psi(q)\Psi(-q) \tag{A4}$$

in which Fourier components only interact with themselves, independently contributing to the energy according to the radial distance between the wave vector and the optimal shell $|q| = q_0$.

A modulated concentration wave such as $\Psi(x)$ in eq A2 has "sidebands" with wave vector $\vec{q}_0 \pm \delta\vec{q}$ in addition to the main Fourier component at $\vec{q}_0$, where $\delta\vec{q}$ is the wave vector of the amplitude modulation $a(\delta q)$. The cases corresponding to longitudinal and transverse modulation are shown in Figure 9.

In the Hamiltonian of eq A4, in which each Fourier component (and its conjugate) contributes to the energy independently, the difference between longitudinal and transverse modulation is clear. For longitudinal modulation, the sidebands are displaced by δq in the radial direction away from the optimal shell and so contribute $(\delta q)^2 a(\delta q)\, a(-\delta q)$ to the energy. For transverse modulation, the sidebands are displaced by δq tangent to the optimal shell, so that the radial distance to the shell is only δq^2; then the contribution to the energy becomes $(\delta q)^4\, a(\delta q)a(-\delta q)$.

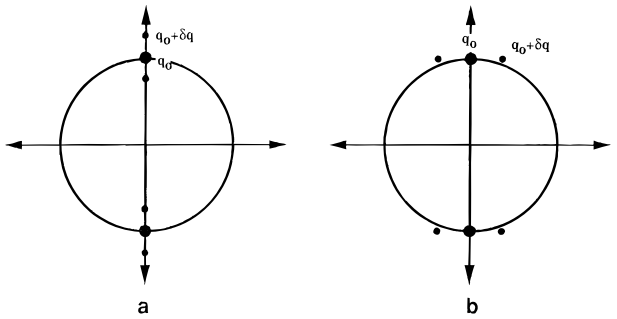

Figure 9. Fourier space representation of modulated lamellar phase in (a) longitudinal and (b) transverse directions.

But this result clearly depends on the absence of any interaction between the main Fourier component and the sidebands, i.e. on the Hamiltonian being quadratic. In other words, the main Fourier component breaks rotational symmetry, so that the energy is permitted to depend on the distance δq from the sidebands to the main peak. Thus the argument leading to eq A3 for the gradient terms is only true to second order in the amplitudes. To higher (e.g., fourth) order, there are terms of the form $a^2(\nabla a)^2$ even for transverse modulations. Since we are considering first-order transitions between lamellar and cylindrical phases, we assume that the amplitudes of the uniform ordered states are large enough that the square-gradient terms are important. This is a simplifying assumption, and it certainly misses some physics. For one thing, the resulting square gradient terms will certainly be anisotropic (which is easy to include in our model, at a phenomenological level). Moreover, the amplitudes of the square gradient terms will vary along an interfacial profile as the ordering amplitudes vary. Finally, as the vicinity of the mean-field second-order critical point at $f = {}^1/_2$ is approached, the ordering amplitudes vanish, and we must recover the gradient expansion of equation A3. These are subjects for future work.

References and Notes

(1) Bates, F. S. *Annu. Rev. Phys.Chem.* **1990**, *41*, 525.
(2) Leibler, L. *Macromolecules* **1980**, *13*, 1602.
(3) Matsen. M.; Schick, M. *Phys. Rev. Lett.* **1994**, *72*, 2660.
(4) Hohenberg, P. C.; Halperin, B. I. *Rev. Mod. Phys.* **1977**, *49*, 435.
(5) Swift, J.; Hohenberg, P. C. *Phys. Rev. E* **1995**, *52*, 1828.
(6) Doi, M.; Edwards, S. F. *The Theory of Polymer Dynamics*; Oxford: New York, 1986.
(7) Fredrickson G. H.; Helfand E. *J. Chem. Phys.* **1988**, *89*, 5890, eq 2.10, which is taken from: Kawasaki, K.; Sekimoto, K. In *Dynamics of Ordering Processes in Condensed Matter*; Komura, S., Ed.; Plenum: New York, 1988.
(8) Liebig, C. M.; Fredrickson G. H. *J. Polym. Sci. Part B* **1996**, *34*,163.
(9) Dalvi, M. C.; Lodge, T. P. *Macromolecules* **1994**, *27*, 5591.
(10) Eastman,C. E.; Lodge,T. P. *Macromolecules* **1994**, *27*, 3487.
(11) Brazovskii, S. A. *Sov. Phys. JETP* **1975**, *85*, 41.
(12) Fredrickson, G. H.; Helfand, E. *J. Chem. Phys.* **1987**, *87*, 697.
(13) Qi, S.; Wang, Z. G. *Phys. Rev. Lett.* **1996**, *76*, 1679.
(14) Fredrickson, G. H.; Binder, K. *J. Chem. Phys.* **1989**, *91*, 7265.
(15) Dai, H. J.; Balsara, N. P.; Garetz, B. A.; Newstein, M. C. *Phys. Rev. Lett.* To be published.
(16) de Gennes, P. G; Prost, J. *The Physics of Liquid Crystals*, 2nd. ed.; Clarendon Press: Oxford, England, 1993; Section 7.1.2.

MA961181L